AAPS PharmSciTech, Vol. 19, No. 4, May 2018 (© 2018)
DOI: 10.1208/s12249-018-0962-y

Research Article

Enhancing the Therapeutic Efficacy of Tamoxifen Citrate Loaded Span-Based Nano-Vesicles on Human Breast Adenocarcinoma Cells

Mohammed A. Kassem,[1] Mohamed A. Megahed,[2] Sherif K. Abu Elyazid,[2,3] Fathy I. Abd-Allah,[2,3] Tamer M. Abdelghany,[4] Ahmed M. Al-Abd,[5,6,7] and Khalid M. El-Say[3,8,9]

Received 7 November 2017; accepted 23 January 2018; published online 22 February 2018

Abstract. Serious adverse effects and low selectivity to cancer cells are the main obstacles of long term therapy with Tamoxifen (Tmx). This study aimed to develop Tmx-loaded span-based nano-vesicles for delivery to malignant tissues with maximum efficacy. The effect of three variables on vesicle size (Y_1), zeta potential (Y_2), entrapment efficiency (Y_3) and the cumulative percent release after 24 h (Y_4) were optimized using Box-Behnken design. The optimized formula was prepared and tested for its stability in different storage conditions. The observed values for the optimized formula were 310.2 nm, −42.09 mV, 75.45 and 71.70% for Y_1, Y_2, Y_3, and Y_4, respectively. The examination using electron microscopy confirmed the formation of rounded vesicles with distinctive bilayer structure. Moreover, the cytotoxic activity of the optimized formula on both breast cancer cells (MCF-7) and normal cells (BHK) showed enhanced selectivity (9.4 folds) on cancerous cells with IC_{50} values 4.7 ± 1.5 and 44.3 ± 1.3 μg/ml on cancer and normal cells, respectively. While, free Tmx exhibited lower selectivity (2.5 folds) than optimized nano-vesicles on cancer cells with IC_{50} values of 9.0 ± 1.1 μg/ml and 22.5 ± 5.3 μg/ml on MCF-7 and BHK cells, respectively. The promising prepared vesicular system, with greater efficacy and selectivity, provides a marvelous tool to overcome breast cancer treatment challenges.

KEY WORDS: Box-Behnken design; Breast cancer cells; *In vitro* cytotoxicity; Optimization; Tamoxifen citrate.

INTRODUCTION

Breast cancer is ranked the second death leading malignancy in females (1). It represents 25% of all cancer types and 15% of deaths in women diagnosed with cancer worldwide, where 1.7 million females were diagnosed with breast cancer and 522 thousands cases died due to breast cancer in 2012 (2,3). Uncontrolled growth of cancerous cells in the mammary epithelial tissues is the main characteristic of breast cancer (4). High toxicity and other very serious side effects are the major problems facing cancer patients treated with chemotherapeutic agents (5). Yet, the challenge is how to deliver chemotherapeutic agent to the target cancer site in appropriate therapeutic concentration while avoiding systemic serious non-tolerated side effects (6). One of the major risk factors for breast cancer is the use of hormone replacement therapy, so hormone antagonists are considered one of the most effective treatments for breast cancer (7).

Tamoxifen (Tmx) is one of the selective estrogen receptor modulators (SERMs) showing estrogenic, antiestrogenic and/or mixed effects according to the site of action (8). Tmx acts as estrogen receptor blocker in breast tissue and accordingly; it is one of the most frequently used and effective remedy for estrogen receptor positive (ER^+) breast cancer (9). In clinical studies, Tmx reduced breast cancer mortality rate to one third (10,11). Furthermore, it is recommended as a prophylactic drug for women at high risk of developing breast cancer (12). Tmx citrate oral tablet is the commercially available form and is prescribed in a dose of 10–20 mg/day (13). Despite the widespread use of Tmx citrate oral tablets, it still has a clear low oral bioavailability (≤ 30%) due to its

[1] Department of Pharmaceutics and Industrial Pharmacy, Cairo University, Cairo, Egypt.
[2] Department of Pharmaceutics and Pharmaceutical Technology, Egyptian Russian University, Cairo, Egypt.
[3] Department of Pharmaceutics and Industrial Pharmacy, Al-Azhar University, Cairo, Egypt.
[4] Department of Pharmacology and Toxicology, Al-Azhar University, Cairo, Egypt.
[5] Department of Pharmacology and Toxicology, King Abdulaziz University, Jeddah, Saudi Arabia.
[6] Pharmacology Department, Medical Division, National Research Center, Giza, Egypt.
[7] Biomedical Research Section, Nawah Scientific, Cairo, Egypt.
[8] Department of Pharmaceutics, King Abdulaziz University, Jeddah, Saudi Arabia.
[9] To whom correspondence should be addressed. (e–mail: kelsay1@kau.edu.sa)

reduced water solubility and significant hepatic first-pass effect (14–17). Thrombocytopenia, leucopenia, hemolytic anemia, hepatic necrosis, multifocal hepatic fatty infiltration, oxidative stress-mediated hepatotoxicity, and endometrial cancer are serious adverse effects of long-term therapy with Tmx (18). These serious adverse effects made a great need to develop new drug delivery systems for Tmx. These drug delivery systems aim to maximize Tmx therapeutic effect and minimize its undesirable adverse effects by targeting the drug action to the desired site of action without affecting other organs.

Nanotechnology has proven a marvelous success in emerging new diagnostic tools and therapeutics for different diseases, especially cancer (19,20). Targeting of anticancer drugs to target cancer cells can be successfully done by using nanocarriers (NCs). So, they have a very important role in cancer treatment (21). Targeting of chemotherapeutics can be done through attaching NCs to specific ligands which are able to bind to specific surface receptors or antigens that present on cancer cells (22–24). They can be formulated with optimum size and surface characters in order to increase the biodistribution and prolong time in circulation. Also, they can modify kinetic properties of drugs without affecting drug activity and deliver drugs to tiny areas within the body. Enhanced permeability and retention is the main advantage of NCs for delivering chemotherapeutic agents at higher concentrations in cancerous tissue than normal non-cancerous tissues (25). Nonionic surfactants based nanocarriers (niosomes) are considered one of the promising drug delivery systems used for these purposes (26,27). Niosomes have been displayed as promising NCs, and it was proven that niosomes had reduced toxic side effects of the anticancer drug, paclitaxel (28). Niosomes, as a unique drug delivery system, are formed by self-assembly of the dried thin film of surfactant upon aqueous hydration into closed bilayer structure in the presence of cholesterol (29,30). Niosomal bilayer structure makes niosomes capable of encapsulation of hydrophilic drugs in the hydrophilic core and hyrophobic drugs in the bilayer membrane (31). Niosomes have many advantages such as (1) they act as a drug reservoir for controlled drug release, (2) they show high stability over long storage periods, (3) they have low toxicity and high compatibility with biological systems, (4) they improve the oral bioavailability of drugs with low bioavailability, (5) they are effectively used to deliver various drugs to the targeted organs, and (6) they can change half-lives and metabolism of anticancer drugs and so, show a good accumulation within tumors (32).

The aim of this research is to develop an optimized stable Tmx-loaded niosomal formulation with optimum particle size, zeta potential, entrapment efficiency, and cumulative drug release percentage after 24 h for increasing the efficacy and selectivity of Tmx against breast cancer and with higher safety against normal cells and thus, reducing possible side effects.

MATERIALS AND METHODS

Materials

Tamoxifen citrate was a gift sample from Chemische Fabrik Berg (GmbH, Germany). Sorbitan monostearate (Span 60) and sorbitan laurate (Span 20) were purchased from Merck Schuchardt OHG (Hohenbrunn, Germany). Sorbitan monopalmitate (Span 40) was obtained from Sigma-Aldrich Chemie GmbH (Steinheim, Germany). Potassium phosphotungstate was obtained as a gift from National Research Center, pharmaceutical technology department (Cairo, Egypt). Cholesterol from lanolin, dicetyl phosphate (DCP), dimethyl sulfoxide, and 3-(4, 5-dimethylthiazol-2-yl)-2, 5-diphenyltetrazolium bromide salt (MTT) were procured from Sigma-Aldrich Company (St. Louis, MO). Chloroform HPLC was purchased from Panreac Quimica SA (Barcelona, Spain). Methyl alcohol absolute, ChromAR® HPLC was obtained from Macron fine chemicals (PA, USA).

METHODS

Determination of Variables Through Preliminary Study

Preliminary study was performed by preparing different Tmx-loaded niosomal formulations. Two types of nonionic surfactants, sorbitan monoesters (Span™; Sp), were used for preparation of Tmx niosomes, namely Span 40 and Span 60 (33). Cholesterol (Chol) was used with spans as stabilizer for niosomal formulation and to increase membrane rigidity, as it has the capability to cement the leaking space in the bilayer membranes (34,35). DCP was added as a negative charge-inducing agent to decrease the possibility of aggregation and stabilize the niosomal vesicular system, leading to formation of stable colloidal dispersion (36). Eight Tmx-loaded niosomal formulations were prepared for the preliminary study. Four preparations were prepared without adding DCP using mentioned two span types with 2 M ratios as follows, Sp: Chol, (1:1) and (2:1). While the other four preparations were prepared with the addition of DCP with 2 M ratios as follows: Sp: Chol: DCP, (1:1:0.15), and (2:1:0.15). The study was conducted to evaluate the effect of type of nonionic surfactant used, charge-inducing agent (DCP) and molar ratio (Sp: Chol) on the percentage of drug entrapped, vesicle size and zeta potential of formulated Tmx-loaded niosomes, and finally to decide which factors would be implemented in the optimization of different Tmx niosomes.

Experimental Design

For optimization of Tmx-loaded niosomes, Box-Behnken design (BBD) was used (37,38). The process was optimized to get the three levels of HLB of Span (X_1), cholesterol concentration (X_2), and DCP concentration (X_3), which minimize mean particle size (Y_1) and maximize each of zeta potential (Y_2), entrapment efficiency (Y_3), and cumulative release after 24 h (Y_4). HLB of the surfactant, cholesterol concentration, and DCP concentration were chosen as the independent variables to study their effects on Y_1–Y_4. A description of the dependent and independent variables with their levels are given in Table I. A total of 15 experimental runs with triplicate center points were generated and their compositions and the observed responses' values are given in Table II. The mathematical relevancies among the observed responses and the designated factors were explicated, using the statistical package Statgraphics® Centurion XV software, version 15.2.05 (StatPoint, Inc., Warrenton, VA), as polynomial equations and their significance was clarified by ANOVA.

Table I. Independent and Dependent Variables of Box-Behnken Design for Development of Tamoxifen Loaded Niosomal Formulations

Independent variables (factors)	Levels			Units
	Low (−1)	Medium (0)	High (+1)	
X_1: HLB of span	4.7	6.7	8.6	*Value
X_2: Cholesterol concentration	0.5	1	1.5	Molar ratio
X_3: DCP concentration	0.15	0.2	0.25	Molar ratio
Dependent variables (responses)	Units		Goal	
Y_1: mean particle size	nm		Minimize	
Y_2: zeta potential	mV		Maximize	
Y_3: entrapment efficiency	%		Maximize	
Y_4: cumulative drug release	%		Maximize	

*HLB value of span 60 = 4.7, span 40 = 6.7, and span 20 = 8.6

Preparation of Tmx-Loaded Niosomes

Tmx-loaded niosomes and drug-free niosomes were prepared by the thin film hydration method (or called the vortex dispersion method) with some adjustments (37,38). A mixture of 100 mg of Sp, Chol, with or without DCP, were weighed according to the molar ratios investigated (39,40). A constant weight of Tmx (5 mg) was also added to the previous mixture. The mixture was added in the pear-shaped flask of the rotary evaporator, Büchi-M/HB-140, (Flawil, St. Gallen, Switzerland), and dissolved in chloroform, rotated for 10 min, on a water bath at 58–60°C. Chloroform was evaporated slowly and completely removed under vacuum for 30 min to leave a thin dry film of solid mixture deposited on the wall of the flask. Then the thin film was hydrated with a 10-ml distilled water. The flask was allowed to rotate again on the water bath at 58–60°C for 20 min; this step was performed in the presence of seven glass beads of 4 mm diameter for assuring complete hydration of dry thin film (38,39). The dispersion was vortexed for 5 min, sonicated at 55°C for 30 min at 20 kHz, and stored at −20°C till further investigation (41). All formulations' compositions are presented in Table II.

Separation and Washing of Tmx-Loaded Niosomes

The frozen Tmx niosomal dispersion was thawed above the temperature of preparation *viz.*, 58–60°C, as it was reported that the entrapment efficiency was largely improved by freeze-thawing process. Separation of free Tmx from the niosomal dispersion was achieved by refrigerated centrifuge (Centurion Scientific Ltd., Stoughton, UK) at temperature of about 4°C and force of ×10,000*g*. The niosomal pellets were washed by re-dispersion in distilled water, using a vortex mixer, and then centrifuged again. This washing technique was repeated twice to make sure that the un-entrapped drug was no longer present in the void space between the niosomal vesicles (42).

Determination of the Entrapment Efficiency

A weight of 100 mg of the washed vesicles was re-dispersed in a 10-ml distilled water and the amount of Tmx entrapped in niosomes was determined by dissolving 1 ml of redispersed vesicles in 30 ml methanol and sonicated for 10 min. A clear solution was obtained and measured spectrophotometrically at wavelength 276 nm against drug-free niosomes handled with the same procedure, as a blank using UV-Visible spectrophotometer, Jasco V-630 (Tokyo, Japan). Entrapment efficiency was

Table II. Experimental Runs and Observed Values of Responses for BBD

Run	Factors			Responses			
	X_1 (value)	X_2 (M)	X_3 (M)	Y_1 (nm)	Y_2 (mV)	Y_3 (%)	Y_4 (%)
F1	6.65	0.5	0.15	620.9	−25.63	72.09	76.87
F2	6.65	1	0.2	363.6	−38.61	74.13	61.45
F3	6.65	1.5	0.15	704.8	−24.70	63.23	68.34
F4	8.6	1.5	0.2	519.7	−34.84	51.91	75.57
F5	4.7	1.5	0.2	602.0	−26.76	50.04	55.00
F6	6.65	0.5	0.25	320.9	−55.00	86.21	75.30
F7	8.6	0.5	0.2	359.8	−31.69	66.89	83.00
F8	6.65	1	0.2	358.3	−35.62	76.09	62.00
F9	8.6	1	0.15	477.1	−21.10	64.00	66.00
F10	4.7	1	0.25	399.8	−52.63	91.06	58.90
F11	6.65	1.5	0.25	751.5	−35.76	63.91	60.56
F12	4.7	1	0.15	657.6	−28.25	70.21	63.45
F13	4.7	0.5	0.2	575.5	−46.76	86.55	65.00
F14	6.65	1	0.2	375.4	−30.78	72.68	63.90
F15	8.6	1	0.25	473.2	−28.54	64.34	68.00

expressed as shown in Eq. 1 (43,44).

$$\text{Entrapment efficiency}\,(\%) = \frac{\text{Amount of Tmx entrapped}}{\text{Total amount of Tmx added}} \times 100 \quad (1)$$

Characterization of Tmx-Loaded Niosomes

Determination of the Particle Size and Zeta Potential

The particle size distribution by intensity and zeta potential of Tmx-loaded niosomes for all prepared formulations were measured at room temperature using dynamic light scattering (DLS) based on laser diffraction (NICOMP™ 380 ZLS NICOMP particle sizing system, Santa Barbara, California, USA) equipped with a 5 mW laser with a wavelength output of 632.8 nm. Polydispersity index (PI), as indication for the uniformity of vesicles' size distribution in the formulation, was also obtained. The value of particle diameter and zeta potential was the average of 3-cycle determinations of the mean particle diameter.

In Vitro Release Study of Tmx-Loaded Niosomes and Kinetic Treatment

The dialysis membrane method, as designated in previous studies (33,45), was implemented to study Tmx release profile from all niosomal formulations (F1–F15). A suitable volume (3 ml) of the tested niosomal dispersion was wrapped in dialysis bag (MWCO 13000) with 5 cm length and 2.1 cm wide. The dialysis bag was then dipped in a 50-ml phosphate buffer (pH 7.4) containing 0.1% (*w*/*w*) Tween 80 as a medium of release that was 3–5 greater than the saturation solubility of Tmx to ensure the sink condition (solubility in phosphate buffer pH 7.4 containing 0.1% Tween 80 is 0.32 mg/ml) (46,47). The release study was performed using rotary shaker (model GLF 3203; Hilab, Düsseldorf, Germany). The shaker was adjusted to 150 strokes/min and temperature at 37°C (48). A sample of 3 ml was withdrawn and substituted with an equal volume of fresh medium at programmed time intervals 0.5, 1, 2, 4, 6, 8, 12, and 24 h. The release of free Tmx was performed at the same conditions as a control. Samples were analyzed spectrophotometrically at a wavelength of 279 nm to determine the concentration of Tmx in all samples based on the standard calibration curve. Results were stated as percentage of cumulative drug release of three replicates. To obtain the kinetics of release, data obtained were tailored to the release kinetic models (zero, first, or second order and Higuchi model) by comparing the correlation coefficients' values to select the best fitted release model. Also, Korsmeyer-Peppas model was applied to determine the mechanism of drug release from the niosomal formulations.

Prediction, Preparation, and Characterization of the Optimized Formula

BBD was successfully adopted and the experiments were designed by choosing the input variables with the selected levels. Response surface methodology (RSM) evolved for responses showed the effect of each input parameter and its interaction with other parameters which was utilized for predicting and obtaining the optimized Tmx niosomal formula using Statgraphics software. The optimized formula was prepared and evaluated by measuring its vesicle size, zeta potential, entrapment efficiency percent, and cumulative percent of drug release after 24 h.

Differential Scanning Calorimetry

Differential scanning calorimetry (DSC) was employed to study the possible interaction between Tmx and the niosomes forming components (49). Shimadzu DSC-50 differential scanning calorimeter (Shimadzu Corporation, Kyoto, Japan) was adjusted at heating rate of 5°C/min over a temperature range of 20–250°C with nitrogen purging (100 ml/min). DSC thermograms of the optimized formula and all individual niosomal forming components as well as the free Tmx were reported (50–52).

Transmission Electron Microscopy

Transmission electron microscope (TEM) was used to confirm the formation of the bilayer structure of the vesicles and determine accurately their sizes using transmission electron microscopy (Jeol, JEM-2100; Japan). To allow some of the particles to stick to the carbon substrate, one drop of the niosomal dispersion was smeared to a carbon-coated grid and left for 1 min. A piece of filter paper was used to remove the excess of the dispersion. One drop of the staining solution (1% phosphotungstic acid solution) was added and the excess of the solution was removed by adsorbing the liquid with the tip of a filter paper. The sample was left in air to dry to be examined under electron microscope (53,54).

Stability Study of the Optimized Formula

The optimized Tmx-loaded niosomes were prepared and evaluated for their stability by determination of the entrapment efficiency, mean particle size, and zeta potential. The stability of the optimized Tmx-loaded niosomes was carried out in two different storage conditions as mentioned in ICH (International Conference of Harmonization) stability guidelines. The formulation was introduced into glass sealed vials and stored at refrigerator temperature (4°C) and at room temperature (25°C) for a period of 3 months (55). Samples were collected at predetermined time intervals (0, 1, 2, and 3 months) and examined for the effect of storage on the particle size, zeta potential, and the drug leakage from Tmx-loaded niosomes. The percentage of Tmx retained in niosomes after each period of time was determined from the Eqs. 2 and 3 (50).

$$\%\ \text{of Tmx retained} = \frac{\%\text{of Tmx entrapped after storage}}{\%\text{of Tmx entrapped before storage}} \times 100 \quad (2)$$

$$\%\ \text{of Tmx leakage} = 100 - \%\ \text{of Tmx retained} \quad (3)$$

In Vitro Cytotoxicity Study

In this study, *in vitro* cytotoxicity against human breast adenocarcinoma cell lines (MCF-7) and baby hamster kidney

fibroblast cell lines (BHK) representing the normal cells was carried out for the optimized Tmx-loaded niosomes in addition to the free Tmx. The concentration that induces 50% growth inhibition from the optimized formula was calculated using Emax model and compared with this of the free Tmx.

Cell Culture

Human breast adenocarcinoma cells (MCF-7) and baby hamster kidney fibroblast cells (BHK), were initially acquired from American type culture collection (ATCC, Manassas, VA, USA) and grown in the tissue culture lab of the Egyptian company for production of vaccines, sera, and drugs (Vaccera, Giza, Egypt). The cells were transported to our laboratory and preserved in Roswell Park Memorial Institute media (RPMI-1640). Media were supplemented with streptomycin (100 μg/ml), penicillin 100 (i.u./ml), and heat-inactivated fetal bovine serum (10% *v*/*v*) in a humidified, 5% (*v*/*v*) CO_2 atmosphere at 37°C (56). Cells were reserved in exponential growth phase (sub-confluence) by sub-culturing at confluence below 70%.

Cytotoxicity Assay (MTT)

Exponentially growing cells were trypsinized and seeded in 96-well plates with cell densities of 1000–2000 cells/well. Cells were incubated overnight in a humidified chamber at 37°C to attach, and then were subjected to serial concentrations of free Tmx and the optimized Tmx-loaded niosomes for 72 h.

Blank niosomal formulation free from drug was also made as a control. At the end of the treatment period, media were discarded, and cells were incubated with MTT solution (5%) for 2 h. MTT solution was removed and formazan crystals were dissolved in acidified isopropanol for 30 min at room temperature with continuous shaking. Absorbance was measured at 570 nm using Epoch-2C plate reader (Bio Tek Inc., Winooski VT, USA). Cell viability was expressed relative to the control untreated cells and the concentrations induced 50% growth inhibition (IC_{50}) were calculated using E_{max} model (Eq. 4) (57,58)

$$\%\text{Cell viability} = (100-R) \times \left(1-\frac{[D]^m}{K_d^m + [D]^m}\right) + R \qquad (4)$$

where R is the resistance fraction, (D) is the concentration of drug, K_d is the concentration of drug that makes the reduction of the maximum inhibition rate by 50%, and m is the "Hill-type coefficient." IC_{50} is defined as the concentration of the drug required to decrease color intensity by 50% of that of the control (59).

Red Blood Cell Hemolysis Assay

To assess the biocompatibility of the optimized formula (O.F. Tmx), RBC's hemolytic assay was undertaken and compared to free Tmx. Briefly, blood sample was drawn from an anonymous human donor, directly into K2-EDTA-coated vacutainer tubes to prevent coagulation. The blood sample was then centrifuged at ×500*g* for 5 min to remove the plasma and to ensure no signs of hemolysis. Plasma was discarded and remaining RBCs were suspended in phosphate buffered saline (PBS) and washed trice. The RBC's suspension was diluted 1:50 in PBS and 150 μl of diluted erythrocytes was transferred to each well in 96-wells plate and incubated with the serial concentrations of free Tmx, O.F. Tmx, and PBS as negative control or triton X 20% as positive control for 1 h at 37°C. The plate was then centrifuged for 5 min at ×500*g* to pellet intact erythrocytes and the supernatant was transferred to a new 96-wells plate; absorbance was measured at 450 nm using epoch 1-C plate reader (Bio Tek, Inc., Winooski VT, USA). To calculate hemolysis percent, triton X absorbance was considered as 100% hemolysis and all values were normalized accordingly. Data were represented as mean ± standard error of mean (SEM) for three independent experiments (60).

RESULTS AND DISCUSSION

Variables Affecting Entrapment Efficiency of Tmx-Loaded Niosomes

From the preliminary study, it was clear that all Tmx-loaded niosomes containing the negative charge-inducing agent, DCP, exhibited higher entrapment efficiency than those had not DCP at the molar ratios investigated. This could be explained by the fact that inclusion of charged molecule such as DCP into niosomes resulting in an increase in stability of niosomal systems. Also, it could be explained by the possible attraction forces between the cationic drug (Tmx) and DCP. The obtained results were in a good agreement with previous studies that investigated the effect of charged molecules on entrapment efficiency of niosomal systems (61). The second important variable that affected the entrapment efficiency of Tmx-loaded niosomes was the cholesterol concentration, where all Tmx niosomal formulae with molar ratio 2:1 (Sp: Chol) showed higher entrapment percentage than the corresponding formulae with molar ratio 1:1 (Sp: Chol). It was found that addition of cholesterol increased the amount of drug entrapped up to the optimal concentration of cholesterol (62,63). Additional increase of cholesterol amount reaching 1:1 M ratio, reduced the amount of drug entrapped owing to the disruption of the bilayer structure. This can be explained by two reasons; firstly, the relative high lipophilicity of Span 60 with minor critical packing parameter. So, only small amount of cholesterol are essential to achieve the optimum membrane curvature for the niosomal structure. Secondly, greater amounts of cholesterol may competitively replace the drug from the packing space within the bilayer as the amphiphiles assemble into the vesicles. The third variable affecting the entrapment efficiency was the span type (HLB), where all Tmx-loaded niosomes with or without DCP, with 2 M ratios (1:1) or (2:1), prepared using span 60 (lower HLB 4.7) showed greater entrapment efficiency percentage than the corresponding formulae prepared using span 40 (higher HLB 6.7) (64,65). Moreover, the freeze-thawing cycles enhance the trapping efficiencies of MLVs by breaking them and formation of more homogenous vesicles population that appear to be largely unilamellar (66). Also, an increase in entrapment efficiency after freeze thawing has also been observed using liposomes. Another mechanism behind this higher entrapment efficiency might be due to the formation of ice crystals in the external

water regions during cooling to 20°C while the internal water crystallizes at much lower temperatures (67).

Variables Affecting the Particle Size and Zeta Potential of Tmx-Loaded Niosomes

The results obtained from the preliminary study revealed that addition of DCP to all Tmx niosomal formulae led to decrease the particle size and increase the zeta potential. This could be explained by the fact that the chemical structure of Tmx citrate contains amine group attached to citrate anion which leads to formation of positive charge on the quaternary amine making the Tmx base behaves as cationic drug carrying a positive charge. So, it was expected that Tmx when encapsulated in niosomes not containing DCP would lead to neutralization of the surface negative charge on niosomes surface leading to decreasing niosomal negative surface charge and thus increasing the attraction forces between niosomal particles leading to possible aggregation could occur which could lead to increasing particle size and decreasing zeta potential of Tmx niosomes not containing DCP. Similar effect was shown when stearylamine, a positive charge inducer that contains also a positively charged amine group, was added to different niosomal formulations. This possible aggregation for Tmx-loaded niosomes not containing DCP could be overcome by the use of probe sonication (68), but the niosomal formulations still had the possibility to re-aggregate due to lower negative surface charge. So, the addition of DCP could increase the surface negative charge of niosomes and neutralize the effect of cationic drug (Tmx) leading to decrease the possibility of aggregation and finally minimize the particle size and maximize the zeta potential which led to more stable niosomal dispersion. Another variable affecting particle size was the cholesterol concentration which increased hydrodynamic diameters of the vesicles and hence increase their particle size. Cholesterol would be more likely to increase the number of bilayers since it has little effect on the charge at the bilayer surface and interlayer separation (40,69,70). Finally, it was observed that Tmx-loaded niosomes prepared using span 60 (lower HLB) showed higher particle size than those of span 40 (higher HLB). These results were in agreement with previous studies which reported that surfactants with lower HLB value and longer alkyl chains, usually form larger vesicles (71).

Response Surface Methodology for the Optimization of Tmx-Loaded Niosomes

Estimation of the Quantitative Effects of the Factors

Multiple regression analysis using Statgraphics software with two-way ANOVA was adopted for statistical analysis of BBD formulae. The estimated factor effects and associated *p* values on the four responses from ANOVA were presented in Table III. Figure 1 showed the main effect plots of the factors on the four investigated responses. The effect of any factor is considered significant if the effect differs from zero and the p value < 0.05. A synergistic effect (direct relationship between the factor effect and the investigated response) was specified by a positive sign, while an antagonistic effect (inverse relationship between the factor effect and the investigated response) of the factor was denoted by a negative sign as shown in Table III. Also, Pareto charts in Fig. 2 displayed these relationships among the factors and the responses and their significant ones. In addition, 3D response surface plots in Fig. 3 revealed the effect of all factors on the responses over the studied levels of factors.

It was clear that HLB of surfactant (X_1) had a significant synergistic effect on the cumulative drug release percentage after 24 h (Y_4) with p value of 0.0115. On the other hand, HLB of surfactant (X_1) had a significant antagonistic effect on zeta potential (Y_2) and entrapment efficiency (Y_3) with p values of 0.0374 and 0.0085, respectively. The cholesterol concentration (X_2) was found to have a significant synergistic effect on the particle size (Y_1) with p value of 0.0093. While, it had a significant antagonistic effect on the zeta potential (Y_2), the entrapment efficiency (Y_3), and the cumulative drug release percentage after 24 h (Y_4) with p values of 0.0374, 0.0085, and 0.0252, respectively. The concentration of DCP (X_3) showed a significant synergistic effect on zeta potential (Y_2) and entrapment efficiency (Y_3) with p values of 0.0031 and 0.0309, respectively. On the other hand, X_3 had a significant antagonistic effect on the particle size (Y_1) with p value of 0.0294. Also, it was noticed that the quadratic term of X_2 had a significant synergistic effect on the particle size (Y_1) and the cumulative drug release percentage after 24 h (Y_4) with p values of 0.0112 and 0.0372, respectively. On the other hand, it showed a significant antagonistic effect on the entrapment efficiency (Y_3) with p value of 0.0491. Finally, it was also noticed that the quadratic term of X_3 and the interaction term X_2X_3 had a significant synergistic effect on the particle size (Y_1) with p values of 0.0168 and 0.0348, respectively.

Effects on the Mean Particle Size (Y_1)

The mean particle size of all niosomal formulae (Y_1) was in the range from 320.9 nm for F6 to 751.5 nm for F11. The polydispersity index (PI) of all niosomal formulations ranged from 0.19 for F6 to 0.54 for F13 which indicated a uniform size distribution of niosomal dispersions. From the obtained results, it was clearly observed that X_2 (cholesterol concentration) was the main factor which was responsible for the difference in the mean particle size of Tmx-loaded niosomes as depicted in Figs. 1 and 2. It was observed that cholesterol concentration (X_2) had a significant direct relationship (synergistic effect) on the particle size (Y_1). A clear example for the effect of cholesterol on the particle size was the difference in the particle size between F6 and F11 where, at the same level of X_1 and X_3, an increase in the ratio of cholesterol from 0.5 to 1.5 led to rise in the mean particle size from 320.9 to 751.5 nm. The same finding was observed in the particle size of F1 and F3, where it increased from 620.9 to 704.8 nm by increasing the ratio of cholesterol from 0.5 to 1.5 at the same level of X_1 and X_3. Moreover, this could be confirmed by the increase of the particle size from 575.5 to 602 nm for F13 and F5, respectively due to increase in the ratio of cholesterol from 0.5 to 1.5. This finding was in accordance with the results obtained in previous studies for the effect of cholesterol amount on the mean particle size of niosomes (69,72). On the other hand, it was noticed that DCP concentration (X_3) had a significant antagonistic effect on the mean particle size (Y_1). A clear example for the effect of

Table III. Estimated Effects of Factors Associated *p* Values for Responses (Y_1–Y_4)

Factors	Y_1		Y_2		Y_3		Y_4	
	Factor effect	*p* value	Factor effect	*p* value	Factor effect	*p* value	Factor effect	*p* value
X_1	−101.275	0.0635	3.396	0.0374*	−12.680	0.0085*	12.555	0.0115*
X_2	175.225	0.0093*	3.396	0.0415*	−20.662	0.0010*	−10.175	0.0252*
X_3	−128.750	0.0294*	3.396	0.0031*	8.997	0.0309*	−2.975	0.3985
X_1^2	50.883	0.4543	4.999	0.6209	−9.410	0.0880	1.0125	0.8395
X_1X_2	66.700	0.3189	4.803	0.0609	10.765	0.0532	1.285	0.7894
X_1X_3	126.950	0.0891	4.803	0.1381	−10.255	0.0616	3.275	0.5047
X_2^2	246.083	0.0112*	4.999	0.6186	−11.495	0.0491*	13.372	0.0372*
X_2X_3	173.350	0.0348*	4.803	0.1150	−6.720	0.1766	−3.105	0.5261
X_3^2	221.433	0.0168*	4.999	0.6901	5.615	0.2624	2.262	0.6536

X_1 is the HLB of surfactant (value), X_2 is the cholesterol molar ratio, and X_3 is the charge-inducing agent DCP molar ratio. X_1X_2, X_1X_3, X_2X_3 are the interaction terms between the factors. X_1^2, X_2^2, X_2^3 *are the quadratic terms of the factors.* Y_1 *is the mean vesicle size (nm),* Y_2 *is the zeta potential,* Y_3 *is the entrapment efficiency percentage, and* Y_4 *is the percentage of Tmx cumulative release after 24 h*

* Significant effect of factors on individual responses

DCP on the particle size was the difference in particle size between F12 and F10 where, at equal level of X_1 and X_2, an increase in the ratio of DCP from 0.15 to 0.25 led to the decrease in the mean particle size from 657.6 to 399.8 nm. These results could be explained by the neutralizing effect of DCP for the cationic drug and thus decreasing the possibility for aggregation so, decreasing the particle size.

Effects on Zeta Potential (Y_2)

Zeta potential of all niosomal formulations (Y_2) was in the range from −21.1 mV for F9 to −55 mV for F6. It was clearly observed that X_3 (DCP concentration) was the major factor responsible for the difference in zeta potential of Tmx-loaded niosomes as shown in Figs. 1 and 2. It was observed that DCP concentration (X_3) had a significant direct effect on the zeta potential (Y_2). An increase in the concentration of DCP from 0.15 to 0.25, at the same level of X_1 and X_2, led to the increase (knowing that increasing the value with neglecting the negative sign) in zeta potential from −25.63 to −55 mV for F1 and F6, respectively. The same finding was observed in F12 and F10 by increasing the zeta potential from −28.25 to −52.63 mV, respectively. This postulation could be attributed to the chemical structure of Tmx which carry positive charge on the quaternary amine group. This positive charge has been neutralized by addition of DCP and then increasing the negative charge on the surface by increasing the DCP concentration in the formulation. Also, both HLB value (X_1) and cholesterol concentration (X_2) were found to be responsible for the difference in the zeta potential. It was observed that HLB value (X_1) had a significant antagonistic effect on the zeta potential (Figs. 1, 2, and 3). This was obvious from the difference in zeta potential between F7 and F13, where at the same level of X_2 and X_3, a reduction in HLB value from 8.6 to 4.7 led to the increase in the zeta potential from −31.69 to −46.76 mV. The same effect was found for cholesterol concentration (X_2) on the zeta potential as the potential was increased from −26.76 to −46.76 mV for F5 and F13, respectively by decreasing the cholesterol concentration from 1.5 to 0.5 at the same level of X_1 and X_3. This could be explained by the effect of cholesterol in increasing niosomal

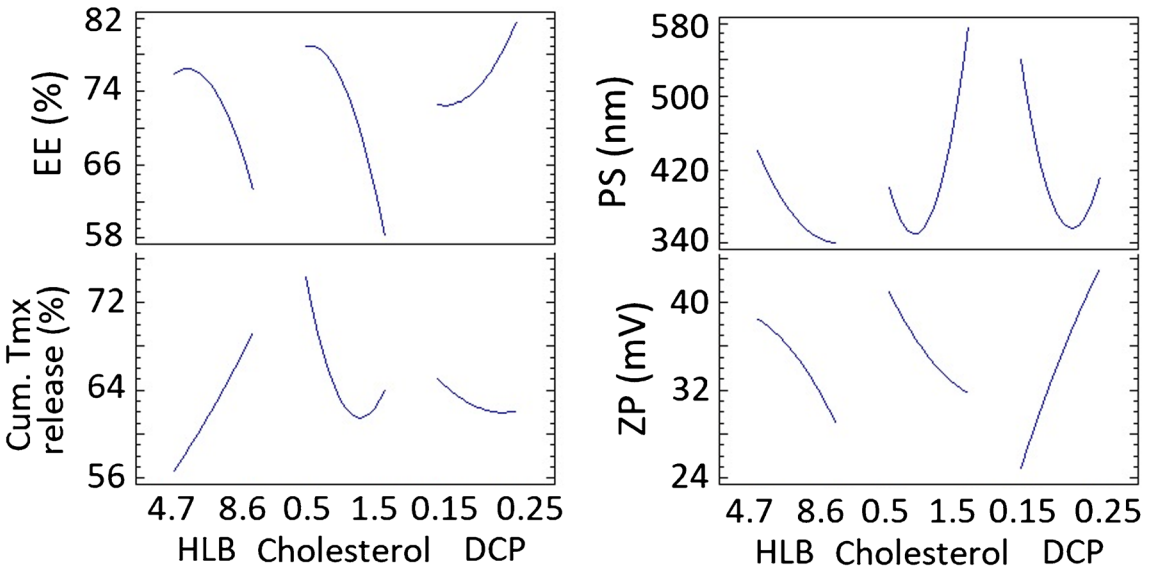

Fig. 1. Main effect plots showing the effects of the investigated factors on all responses (Y_1–Y_4)

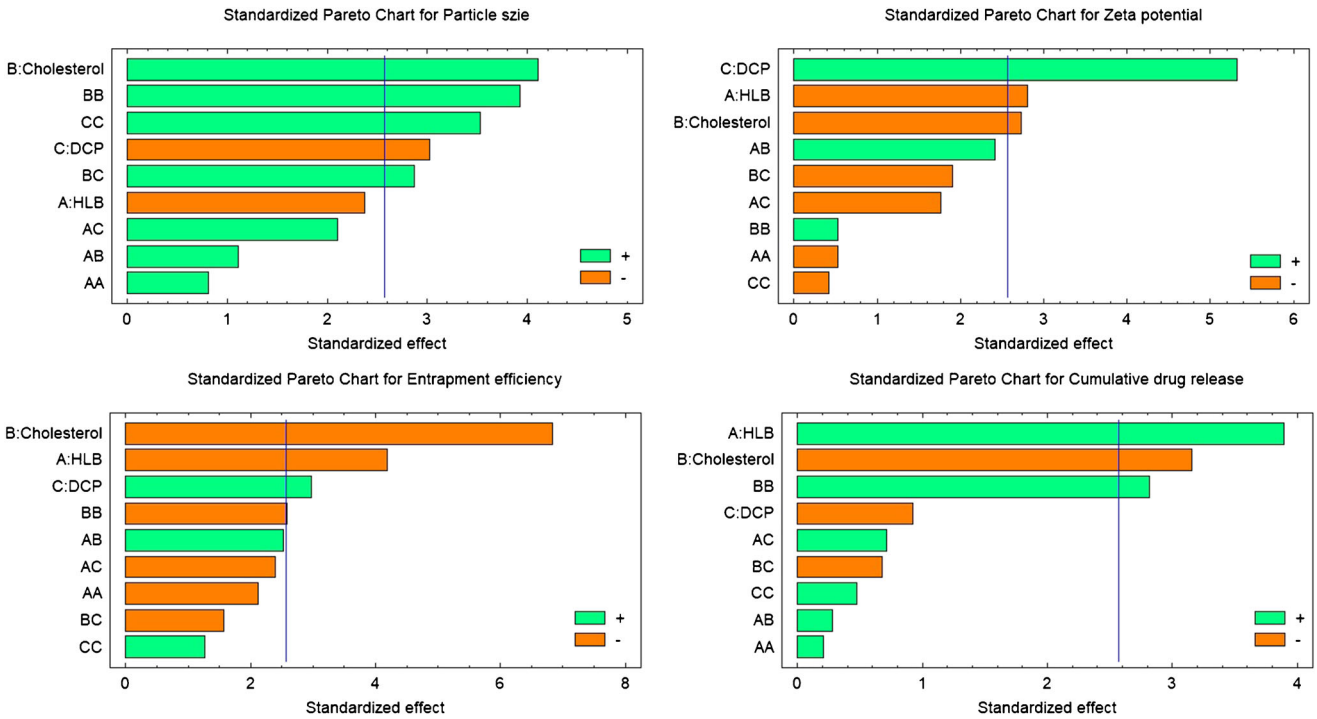

Fig. 2. Standardized Pareto charts showing the effects of the investigated factors on all responses (Y_1–Y_4)

membrane rigidity and stability which in turn was reflected to increase zeta potential and stability of niosomal system (39).

Effects on the Entrapment Efficiency (Y_3)

The entrapment efficiency of all niosomal formulations (Y_3) was ranged from 50.04 to 91.06%. This variation in the entrapment efficiency reflected the good selection of the variables and their levels. It was clearly observed that all variables affect significantly the entrapment efficiency of niosomes. Both X_1 and X_2 have an inverse relationship while X_3 has a direct one as depicted in Figs. 1 and 2. Figures 1, 2, and 3 displayed that the leading factor which was responsible for the difference in the entrapment efficiency of Tmx-loaded formulae was X_2 (cholesterol concentration). At the same level of X_1 and X_3, a decrease in the concentration of cholesterol from 1.5 to 0.5 increased the entrapment efficiency from 50.04 to 86.55% for F5 and F13, respectively. Also, increasing the cholesterol concentration from 0.5 to 1.5 led to decrease the percent of drug entrapped from 66.89 to 51.91% for F7 and F4, respectively. This postulation was closely matched with what was stated in previous studies (73). where the highest entrapment was achieved when niosomes were prepared using surfactant and cholesterol at molar ratio of 2:1. So, increasing the cholesterol concentration led to decrease the entrapment efficiency (74). Also, HLB of Span

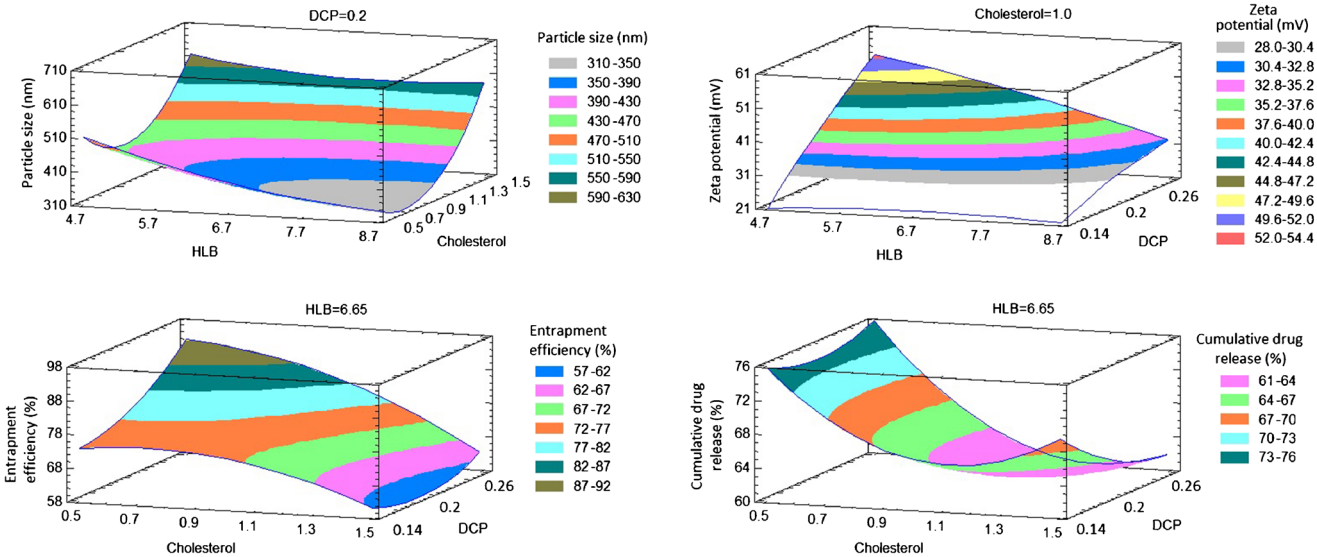

Fig. 3. Estimated response surface plots for the effects of the investigated factors on all responses (Y_1–Y_4)

affected significantly the entrapment efficiency (Y_3). As the HLB value increased from 4.7 in F10 to 8.6 in F15, the percentage of Tmx entrapped would be decreased from 91.06 to 64.34%. The same finding was revealed in F13 and F7, where increasing HLB value from 4.7 to 8.6, without changing X_2 and X_3, decreased the percentage of drug entrapped from 86.55 to 66.89%, respectively. These results could be explained by increasing the alkyl chain length in span 60 (lower HLB) led to higher entrapment efficiency than that observed with span 40 and span 20 (higher HLB) (33,42). On the other hand, it was observed that DCP concentration (X_3) showed a significant direct effect (synergistic effect) on the entrapment efficiency (Y_3). A clear example for the effect of DCP concentration on the entrapment efficiency was the difference in the entrapment efficiency between F12 and F10, where at similar level of X_1 and X_2, an increase in the molar ratio of DCP from 0.15 to 0.25 led to the increase in the entrapment efficiency from 70.21 to 91.06%. This finding might be explained by the possible attraction forces between negative charge on DCP and the cationic drug (61).

Effects on the Cumulative Percentage of Drug Release (Y_4)

Tmx-loaded niosomes showed variation in the cumulative percentage of Tmx release after 24 h (Y_4) ranged from 55% for F5 to 83% for F7 as shown in Table II and Fig. 4a, b. It was clear that the drug release from all niosomal formulations (F1–F15) followed two phases, an initial rapid release that took about 2 h followed by a sustained release phase for 12 h and maintained as plateau for 24 h. The desorption of the adsorbed drug on the niosomal surface could explain the initial rapid release phase, whereas the diffusion mechanism from swollen bilayers of niosomal vesicles was responsible for the sustained plateau phase (75). This biphasic release pattern was confirmed to be a main behavior of drug release from niosomal vesicles; this had been previously described for some liposomes and niosomes (76,77). From the obtained results, it was clearly observed that X_1 (HLB of the surfactant) had the main effect to cause detectable variation in the cumulative percentage release of Tmx after 24 h from niosomes as demonstrated in Fig. 4a. It was observed that HLB value (X_1) had a significant synergistic effect on the cumulative release percentage after 24 h (Y_4). This was observed by the increase in the cumulative percentage drug released after 24 h from 55 to 60.56%, without changing other variables, by the increase in the HLB value from 4.7 to 6.65 for F5 and F11, respectively. A further increase for the percentage of drug released to 75.57% by increasing the HLB value to 8.6 for F4. This could be explained by increasing the length of alkyl chain of the nonionic surfactant, span 20, 40, and 60, a decrease in the percentage of drug released was observed (78,79). On the other hand, it was observed that cholesterol concentration (X_2) showed a significant antagonistic effect on the cumulative drug release percentage after 24 h (Y_4). At constant variables (X_1 and X_3), increasing the concentration of cholesterol from 0.5 to 1.5 led to decrease in the cumulative drug release percentage after 24 h from 65 to 55% for F13 to F5, respectively as shown in Fig. 4b. This might be due to the fact that cholesterol stabilizes the bilayers, prevents drug leakage, and delays permeation of solutes enclosed in the vesicles (80). Prediction of release mechanisms was attained by using the mathematical models. The results of the *in vitro* release study revealed that Tmx release from niosomes was best fitted to Higuchi release kinetics, as revealed by the highest correlation coefficient (r) values. This conclusion suggested that the Tmx was released from niosomes by a diffusion-controlled mechanism. Korsmeyer-Peppas model revealed that most of niosomal formulations showed Fickian diffusion mechanism for drug release where (n) values ranged from 0.36 to 0.5 except the niosomal formulae (F_2, F_5, and F_{11}) showed non-fickian mechanism with (n) values 0.53, 0.52, and 0.6, respectively. Also, the optimized niosomal formula showed Fickian diffusion mechanism. These results were analogous with the reports of numerous studies (62,79). Higuchi drug release pattern confirmed the fact that niosomes can behave as a drug reservoir for constant drug delivery.

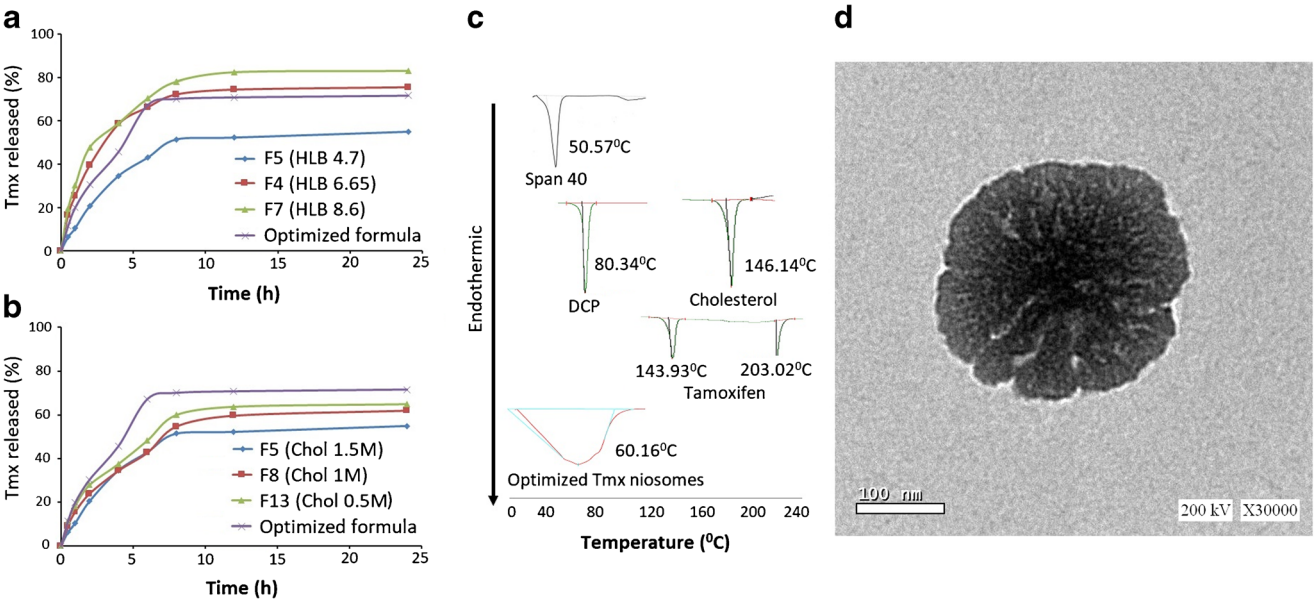

Fig. 4. *In vitro* release profiles for formulations with different HLB (**a**), with different concentrations of cholesterol (**b**) in comparison with the optimized formulation; DSC thermograms of niosomal individual components and the optimized formulation (**c**); Photomicrograph of the optimized Tmx-loaded niosomes formulation by TEM image (**d**)

Also, this sustained release pattern of drug entrapped might refer to the high stability of the niosomal system (40).

Statistical Analysis and Mathematical Modeling of the Experimental Data

Values for the mean vesicle size of niosomes (Y_1), zeta potential (Y_2), entrapment efficiency (Y_3), and the cumulative Tmx release percentage after 24 h (Y_4) were analyzed to produce a mathematical model for each of the mentioned responses. Results of the analysis of multiple regressions for each response variable derived by the best fit model were presented in Eqs. 5–8.

$$\text{Mean vesicle size } (Y_1) = 4966.97 - 279.365\,X_1 - 1729.97\,X_2 - 26798.5\,X_3 + 6.691\,X_1^2 + 34.205\,X_1X_2 + 651.026\,X_1X_3 + 492.167\,X_2^2 + 3467.0\,X_2X_3 + 44286.7\,X_3^2 \quad (5)$$

$$\text{Zeta potential } (Y_2) = -57.402 + 4.906\,X_1 - 22.715\,X_2 + 821.64\,X_3 - 0.346\,X_1^2 + 5.936\,X_1X_2 - 43.436\,X_1X_3 + 5.303\,X_2^2 - 183.1\,X_2X_3 - 422.667\,X_3^2 \quad (6)$$

$$\text{Entrapment efficiency } (Y_3) = 5.687 + 18.203\,X_1 + 15.486\,X_2 + 124.897\,X_3 - 1.237\,X_1^2 + 5.521\,X_1X_2 - 52.589\,X_1X_3 - 22.99\,X_2^2 - 134.4\,X_2X_3 + 1123.0\,X_3^2 \quad (7)$$

$$\text{Cumulative percentage release after 24 h } (Y_4) = 122.199 - 2.569\,X_1 - 55.627\,X_2 - 260.336\,X_3 + 0.133\,X_1^2 + 0.659\,X_1X_2 + 16.795\,X_1X_3 + 26.745\,X_2^2 - 62.1\,X_2X_3 + 452.5\,X_3^2 \quad (8)$$

Preparation of the Optimized Tmx-Loaded Niosomal Formula

BBD is one of response surface methodology (RSM) experimental designs used for optimization and is established on three factor three-level designs with its experimental points being situated on a hypersphere intermediate from the central point (81). BBD helped to get the optimized Tmx-loaded niosomal formula that met our requisite in achieving smallest vesicular size, maximum zeta potential, entrapment efficiency, and cumulative release percentage after 24 h. In order to reach a combination of factor levels that amplify the desirability function, the final optimized parameters were considered and analyzed to compromise among different responses. The reliability of the BBD results was validated by preparing a new formula according to the predicted model and assessed for the responses. The optimized formula was prepared using the obtained optimum values of variables which were 7.87, 0.84, and 0.23 for X_1, X_2, and X_3, respectively. The optimized formula with mentioned optimum variables levels were prepared by thin film hydration technique and characterized as previously mentioned. The predicted values for Y_1, Y_2, Y_3, and Y_4 were 325.51 nm, −35.78 mV, 72.15 and 69%, respectively, whereas the observed responses' values were found to be 310.2 nm, −42.09 mV, 75.45 and 71.70%, respectively.

Characterization of the Optimized Tmx-Loaded Niosomal Formula

Differential Scanning Calorimetry

The DSC thermograms which were shown in Fig. 4c revealed sharp melting endothermic peaks for individual components forming niosomes namely, Span 40, cholesterol, DCP, and pure Tmx. The DSC thermogram of Span 40 exhibited an endothermic peak at 50.57°C which represents its meting point whereas; cholesterol and DCP showed also endothermic peaks at 146.14 and 80.34°C, respectively. In addition, pure Tmx showed endothermic peaks at 143.93 and 203.02°C. As observed in DSC thermogram of the optimized formula, a unique broad peak at 61.16°C with the disappearance of all sharp endothermic peaks of individual components as well as the pure drug Tmx ensured a significant interaction of Tmx with the niosomal components and could explain the high entrapment percent of Tmx into the optimized niosomal formula (49).

Transmission Electron Microscopy

The morphology of the nisomal vesicles were investigated using transmission electron microscope (TEM). The electron micrographs declared the formation of niosomal vesicles with distinct bilayer structure. The vesicles' core was clearly observed with its spherical structure in the photomicrograph as shown in Fig. 4d.

Stability Study of the Optimized Tmx-Loaded Niosomal Formula

Effect of Storage on the Homogeneity of the Optimized Tmx-Loaded Niosomes

The visual observation for the optimized Tmx-loaded niosomes over the period of the stability study (3 months) at the two dissimilar storage temperatures (4 and 25°C) indicated a good physical stability with partial, without coarse particles, sedimentation, no layer separation, and no color change. This could be explained by the fact that the presence of surface charge-inducing agent (DCP) is an important parameter affecting niosomal stability, *i.e.*, high zeta potential

of these systems led to electrostatic repulsion between vesicles which reduced the rate of aggregation and fusion of niosomes during storage (82).

Effect of Storage of the Optimized Formula on the Percent of Drug Leakage, Mean Particle Size, and Zeta Potential

Entrapment efficiency (EE%), percentage of drug leakage, percentage of drug retained, particle size, and zeta potential of the optimized formula stored at two different temperatures, refrigerator temperature at 4°C and room temperature at 25°C, at the end of each month over the storage period were calculated and shown in Table IV.

A storage temperature of 4°C was found to be more suitable to minimize drug leakage from niosomes where the percent of drug leakage after 3 months storage at 4°C was 8.80% while the percent at 25°C was 12.38%. This was expected because the drug leakage increases with temperature increase due to greater fluidity of the niosomal membrane. In addition, the drug leakage was decreased after 3 months compared to the leakage after 2 months. The decrease of drug leakage by storage time might be due to the niosomal system had the ability to stabilize itself by time (55). This finding was in agreement with the literature that mentioned that it was more suitable to store niosomal formulations at refrigerator temperature (55). Also, the stability of the niosomal membrane was increased by the presence of cholesterol which in turn intensely reduced the leakage of the entrapped drug. Moreover, cholesterol produces an optimal lipophilicity which decreases the formation of the transient hydrophilic holes, by diminishing fluidity that account for drug leakage from the niosomal bilayers (83).

The particle size of the original optimized formula was 310.2 nm and increased after 3 months to be 434.9 and 516.7 nm at 4 and 25°C, respectively. These changes in vesicle size might be due to minor fusion and aggregation of the niosomes after storage. In this way, the rate of aggregation and fusion of niosomes might be reduced due to high surface potential and electrostatic repulsion (83).

It was clearly observed that the zeta potential of optimized formula decreased from the initial value of −42.09 mV to be in the range from −38.02 to −30.86 at two different storage temperatures for 3 months. The values of zeta potential of optimized formula were all above −30 in all storage conditions which indicated a very good stability for the optimized formula over 3 months storage at the two different temperatures. These values were assumed to provide adequate repulsion between niosomal vesicles to prevent the aggregation and provide stable colloidal systems. Generally, a niosomal dispersion is considered to be stable when it has a zeta potential value more positive than +30 mV or more negative than −30 mV (84). So, the optimized formula showed high stability over the 3 months storage at both room temperature and refrigerator temperature.

In vitro Cytotoxicity of the Optimized Tmx-Loaded Niosomal Formula

The MTT cell proliferation assay was conducted to study the cytotoxicity of the optimized Tmx-loaded niosomal formulation (O.F. Tmx) on the viability of breast cancer cell lines compared to free Tmx by determining their IC_{50}'s. Free Tmx treatment induced gradual killing effect against MCF-7 cells over concentration range from 0.025 to 250 μg/ml with IC_{50} of 9.0 ± 1.1 μg/ml, and resistant fraction was 0.33 ± 0.1%. Interestingly, niosomal encapsulation significantly ($p < 0.05$) decreased the IC_{50} of free Tmx to 4.7 ± 1.6 μg/ml, and no change in R value was noticed due to formulation (Fig. 5a). It is worth mentioning that prolonged exposure of tumor cells to chemotherapeutic drug might induce treatment resistance (85,86). Yet, any slow release formulation of anticancer agent must be taken carefully to avoid the development of resistance (87). Herein, despite the obvious slower release of Tmx from the niosomal formulation compared to free drug, no significant change in resistance was noticed. Finally, it could be suggested that niosomes significantly interacted with cancer cells with the usual fundamentals and common characteristics of nanoparticles such as niosomes. This kind of cell–nanoparticle interaction was frequently accompanied with internalization through rapid non-specific phagocytosis (47). Nanocarriers have several advantages over free drugs, such as protection from degradation, selective and enhanced absorption into the targeted tissue, and regulate the pharmacokinetic and drug tissue distribution profile. These results were in a good agreement with earlier studies on many nanoparticles and niosomes that showed that the efficacy of drug could be improved by niosomal encapsulation and the dose to be used could be reduced and so the safety would in turn be also improved (48,88–92).

Safety and Biocompatibility Study

In terms of safety, cytotoxic effects of free Tmx and optimized Tmx-loaded formula were assessed against BHK normal cells over the same concentration range (from 0.025 to 250 μg/ml). In contrast to MCF-7 cells, free Tmx exerted

Table IV. Effect of Different Storage Conditions of the Optimized Tmx-Loaded Niosomal Formula on Drug Leakage Percentage, Particle Size, and Zeta Potential

Storage time (month)	Storage temp. (°C)	Entrapment efficiency (%)	Drug retained (%)	Drug leakage (%)	Particle size (nm)	Zeta potential (mV)
0	–	75.45	100	0	310.20	−42.09
1	4	72.40	95.96	4.04	368.20	−38.02
	25	70.41	93.32	6.68	372.20	−33.39
2	4	70.23	93.08	6.92	389.00	−34.31
	25	67.27	89.15	10.85	395.40	−32.16
3	4	68.81	91.20	8.80	434.90	−31.30
	25	66.11	87.62	12.38	516.70	−30.86

significantly ($p < 0.05$) higher cytotoxic profile than the O.F. Tmx against normal BHK cells with IC_{50}'s of 22.5 ± 5.6 μg/ml and 44.3 ± 1.3 μg/ml, respectively (Fig. 5b). Referring to the previously mentioned IC_{50}' values of free Tmx and the O.F. Tmx on MCF-7 cells and BHK cells, it was clear that O.F Tmx showed a greater selectivity (9.4-folds) on cancerous cells than normal cells. On the contrary, free Tmx showed lower selectivity (only 2.5-folds) on cancerous cells. This preferential selectivity of the O.F. Tmx confirmed the greater safety than free drug. The explanation of the greater selectivity of nanocarriers towards cancerous cells may be due to they can be selectively compartmentalized on autophagic sequestration. Autophagy is strongly involved in cancer therapies affirmative outcomes, and nanomaterials can efficiently interrupt the autophagic pathway (21). Additionally, RBC's hemolytic activity was assessed for both free Tmx and optimized Tmx-loaded formula over the same concentration range (from 0.025 to 250 μg/ml). Neither Tmx nor the optimized Tmx-loaded formula exerted any considerable hemolytic activity (less than 5%) up to 25 μg/ml. Exposure of RBC's to 250 μg/ml free Tmx and optimized Tmx-loaded formula resulted in 70.8 ± 1.5% and 16.7 ± 0.95% hemolysis, respectively (Fig. 5c). In summary, we can notice considerable higher safety and biocompatibility for optimized Tmx-loaded formula compared to free Tmx within normal cells (93).

CONCLUSION

Nano-vesicles, as a promising drug delivery system, have shown superb upshots in cancer treatment in last few years. Based on this revolution in fighting cancer, our research succeeded in enhancing the anticancer activity of Tamoxifen citrate by loading it in Span-based nano-vesicles. BBD optimization technique helped in prediction of Tmx niosomal formula which when investigated; it met the demands of the desired responses. The optimized formula Tmx-loaded niosomes showed minimum vesicular size, high zeta potential, maximum entrapment efficiency, and sustained release profile as well as the stability on storage at different temperatures for 3 months. Finally, the cytotoxic activity on cancerous and normal cells revealed the preferential selectivity and greater efficacy of the optimized Tmx-loaded nanosized vesicular system over free Tmx on breast cancer cells. Furthermore, superior safety of the optimized formula on normal cells over free drug was confirmed by little hemolysis effect on RBCs.

COMPLIANCE WITH ETHICAL STANDARDS

Conflict of Interest The authors declare that they have no conflicts of interest.

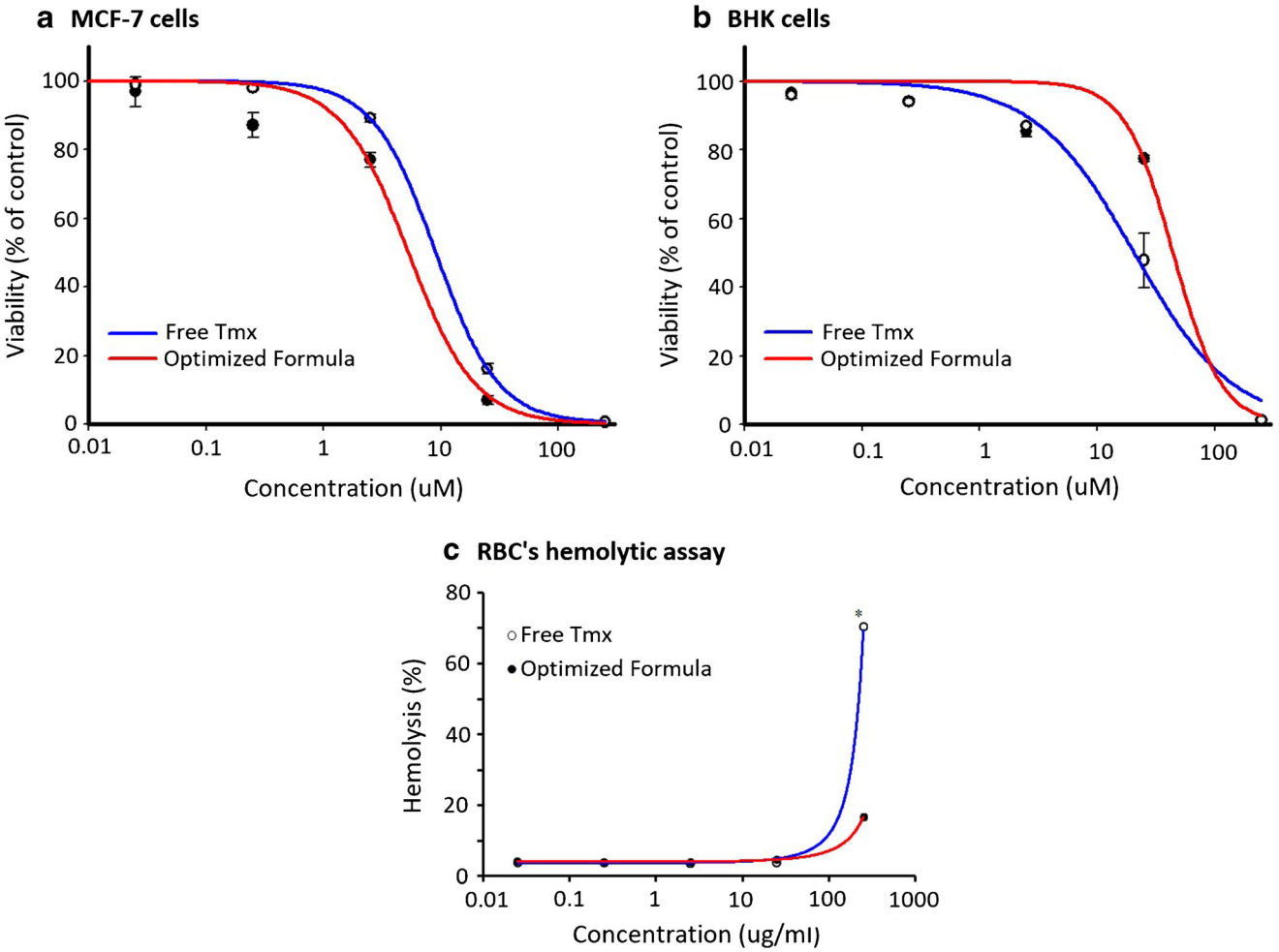

Fig. 5. Dose response relationship (**a**, **b**) and RBC's hemolytic effects (**c**) of free Tmx and optimized formulation against MCF-7 cells (**a**) and BHK cells (**b**)

REFERENCES

1. Jemal A, Siegel R, Ward E, Hao Y, Xu J, Murray T, et al. Cancer statistics, 2008. CA Cancer J Clin [Internet]. 2008;58(2):71–96. Available from: http://doi.wiley.com/10.3322/CA.2007.0010.
2. Torre LA, Bray F, Siegel RL, Ferlay J, Lortet-tieulent J, Jemal A. Global cancer statistics, 2012. CA Cancer J Clin. 2015;65(2):87–108. https://doi.org/10.3322/caac.21262.
3. Ferlay J, Soerjomataram I, Dikshit R, Eser S, Mathers C, Rebelo M, et al. Cancer incidence and mortality worldwide: sources, methods and major patterns in GLOBOCAN 2012. Int J Cancer. 2015;136(5):E359–86. https://doi.org/10.1002/ijc.29210.
4. Lukong KE. Understanding breast cancer – the long and winding road. BBA Clin. 2017;7:64–77. https://doi.org/10.1016/j.bbacli.2017.01.001.
5. Pandey SK, Ghosh S, Maiti P, Haldar C. Therapeutic efficacy and toxicity of tamoxifen loaded PLA nanoparticles for breast cancer. Int J Biol Macromol. 2015;72:309–19. https://doi.org/10.1016/j.ijbiomac.2014.08.012. Elsevier BV.
6. Au JS, Jang SH, Zheng J, Chen CT, Song S, Hu L, et al. Determinants of drug delivery and transport to solid tumors. J Control Release. 2001;74(1–3):31–46. https://doi.org/10.1016/S0168-3659(01)00308-X.
7. Murray AJ, Davies DM. The genetics of breast cancer. Surgery (United Kingdom). 2013;31(1):1–3. Elsevier Ltd.
8. Altmeyer C, Karam TK, Khalil NM, Mainardes RM. Tamoxifen-loaded poly(L-lactide) nanoparticles: development, characterization and in vitro evaluation of cytotoxicity. Mater Sci Eng C. 2016;60:135–42. https://doi.org/10.1016/j.msec.2015.11.019. Elsevier BV.
9. Radin DP, Patel P. Delineating the molecular mechanisms of tamoxifen's oncolytic actions in estrogen receptor-negative cancers. Eur J Pharmacol. 2016;781:173–80. https://doi.org/10.1016/j.ejphar.2016.04.017. Elsevier.
10. Spears M, Bartlett J. The potential role of estrogen receptors and the SRC family as targets for the treatment of breast cancer. Expert Opin Ther Targets. 2009;13(6):665–74. https://doi.org/10.1517/14728220902911509.
11. Jordan VC. Tamoxifen (ICI46,474) as a targeted therapy to treat and prevent breast cancer. Br J Pharmacol. 2006;147(Suppl 1):S269–76.
12. Barron AJ, Zaman N, Cole GD, Wensel R, Okonko DO, Francis DP. Systematic review of genuine versus spurious side-effects of beta-blockers in heart failure using placebo control: recommendations for patient information. Int J Cardiol [Internet]. Elsevier; 2013 Oct 9 [cited 2017 Apr 16];168(4):3572–9. Available from: http://www.ncbi.nlm.nih.gov/pubmed/23796325.
13. Kouchakzadeh H, Shojaosadati SA, Shokri F. Efficient loading and entrapment of tamoxifen in human serum albumin based nanoparticulate delivery system by a modified desolvation technique. Chem Eng Res Des. 2014;92(9):1681–92. Institution of Chemical Engineers
14. Mugundu GM, Sallans L, Guo Y, Shaughnessy EA, Desai PB. Assessment of the impact of CYP3A polymorphisms on the formation of alpha hydroxytamoxifen and N-desmethyltamoxifen in human liver microsomes. Drug Metab Dispos. 2012;40(2):389–96. https://doi.org/10.1124/dmd.111.039388.
15. Zembutsu H. Pharmacogenomics toward personalized tamoxifen therapy for breast cancer. Pharmacogenomics. 2015;16(3):287–96. https://doi.org/10.2217/pgs.14.171.
16. Stevens DM, Gilmore KA, Harth E. An assessment of nanosponges for intravenous and oral drug delivery of BCS class IV drugs: drug delivery kinetics and solubilization. Polym Chem. 2014;5(11):3551–4.
17. Lockhart JN, Stevens DM, Beezer DB, Kravitz A, Harth E. Dual drug delivery of tamoxifen and quercetin: Regulated metabolism for anticancer treatment with nanosponges. J Control Release. 2015;220:751–7. Elsevier B.V.
18. Lee MH, Kim JW, Kim JH, Kang KS, Kong G, Lee MO. Gene expression profiling of murine hepatic steatosis induced by tamoxifen. Toxicol Lett. 2010;199(3):416–24. https://doi.org/10.1016/j.toxlet.2010.10.008. Elsevier Ireland Ltd.
19. Davis ME, Chen Z, Shin DM. Nanoparticle therapeutics: an emerging treatment modality for cancer. Nat Rev Drug Discov. 2008;7(9):771–82. https://doi.org/10.1038/nrd2614.
20. Xin Y, Huang Q, Tang JQ, Hou XY, Zhang P, Zhang LZ, et al. Nanoscale drug delivery for targeted chemotherapy. Cancer Lett. 2016;379(1):24–31. https://doi.org/10.1016/j.canlet.2016.05.023. Elsevier Ireland Ltd.
21. Panzarini E, Inguscio V, Tenuzzo B, Carata E, Dini L. Nanomaterials and autophagy: new insights in cancer treatment. Cancers (Basel). 2013;5(1):296–319. https://doi.org/10.3390/cancers5010296.
22. Bansal D, Gulbake A, Tiwari J, Jain SK. Development of liposomes entrapped in alginate beads for the treatment of colorectal cancer. Int J Biol Macromol. 2016;82:687–95. https://doi.org/10.1016/j.ijbiomac.2015.09.052. Elsevier B.V.
23. Jeong K, Kang CS, Kim Y, Lee Y-D, Kwon IC, Kim S. Development of highly efficient nanocarrier-mediated delivery approaches for cancer therapy. Cancer Lett. 2016;374(1):31–43. https://doi.org/10.1016/j.canlet.2016.01.050. Elsevier Ireland Ltd.
24. Kemp JA, Shim MS, Heo CY, Kwon YJ. "Combo" nanomedicine: co-delivery of multi-modal therapeutics for efficient, targeted, and safe cancer therapy. Adv Drug Deliv Rev. Elsevier B.V. 2016;98:3–18.
25. Patel P, Agrawal YK. Targeting nanocarriers containing antisense oligonucleotides to cancer cell. J Drug Deliv Sci Technol. 2017;37:97–114. https://doi.org/10.1016/j.jddst.2016.12.001. Elsevier Ltd.
26. Ghanbarzadeh S, Khorrami A, Arami S. Nonionic surfactant-based vesicular system for transdermal drug delivery. Drug Deliv. 2014;7544:1–7.
27. Marianecci C, Di Marzio L, Rinaldi F, Celia C, Paolino D, Alhaique F, *et al.* Niosomes from 80s to present: the state of the art. Adv Colloid Interface Sci [Internet]. 2014 Mar [cited 2014 Nov 27];205:187–206. Available from: http://www.ncbi.nlm.nih.gov/pubmed/24369107.
28. Bayindir ZS, Yuksel N. Characterization of niosomes pepared with various nonionic surfactants for paclitaxel oral delivery. J Pharm Technol 2010;99(4):2049–60. Available from: http://www.ncbi.nlm.nih.gov/pubmed/19780133.
29. Shilpa S, Srinivasan BP, Chauhan M. Niosomes as vesicular carriers for delivery of proteins and biologicals. Int J Drug Deliv. 2011;3(1):14–24. https://doi.org/10.5138/ijdd.2010.0975.0215.03050.
30. Bragagni M, Mennini N, Furlanetto S, Orlandini S, Ghelardini C, Mura P. Development and characterization of functionalized niosomes for brain targeting of dynorphin-B. Eur J Pharm Biopharm. 2014;87(1):73–9. https://doi.org/10.1016/j.ejpb.2014.01.006. Elsevier BV.
31. Marianecci C, Di Marzio L, Del Favero E, Cantu L, Brocca P, Rondelli V, et al. Niosomes as drug nanovectors: multiscale pH-dependent structural response. Langmuir. 2016;32(5):1241–9. https://doi.org/10.1021/acs.langmuir.5b04111.
32. Khoee S, Yaghoobian M. Niosomes: a novel approach in modern drug delivery systems. Nanostructures for Drug Delivery. Elsevier Inc.; 2017. p. 207-237. https://doi.org/10.1016/B978-0-323-46143-6.00006-3.
33. Hao Y, Zhao F, Li N, Yang Y, Li K. Studies on a high encapsulation of colchicine by a niosome system. Int J Pharm [Internet]. 2002 Sep [cited 2014 Dec 11];244 (1–2):73–80. Available from: http://www.sciencedirect.com/science/article/pii/S0378517302003010.
34. Manosroi A, Wongtrakul P, Manosroi J, Sakai H, Sugawara F, Yuasa M, *et al.* Characterization of vesicles prepared with various non-ionic surfactants mixed with cholesterol. Colloids Surfaces B Biointerfaces [Internet]. 2003 Jul [cited 2014 Nov 12];30 (1–2):129–38. Available from: http://www.sciencedirect.com/science/article/pii/S0927776503000808.
35. Yeom S, Shin BS, Han S. An electron spin resonance study of non-ionic surfactant vesicles (niosomes). Chem Phys Lipids. 2014;181:83–9. https://doi.org/10.1016/j.chemphyslip.2014.03.004. Elsevier Ireland Ltd.
36. Yoshioka T, Sternberg B, Florence AT. Preparation and properties of vesicles (niosomes) of sobitan monoesters (Span 20, 40, 60, 80) and a sorbitan triester (Span 85). Int J Pharm. 1994;105:1–6.

37. El-Say KMKM, Abd-Allah FI, Lila AE, Hassan AE-SA, Kassem AEA. Diacerein niosomal gel for topical delivery: development, *in vitro* and *in vivo* assessment. J Liposome Res [Internet]. 2016;26(1):57–68. Available from: http://informahealthcare.com/doi/abs/10.3109/08982104.2015.1029495.
38. Kassem MA, El-Sawy HS, Abd-Allah FI, Abdelghany TM, El-Say KM. Maximizing the therapeutic efficacy of imatinib mesylate–loaded niosomes on human colon adenocarcinoma using Box-Behnken design. J Pharm Sci. 2017;106(1):111–22. https://doi.org/10.1016/j.xphs.2016.07.007.
39. El-Ridy MS, Abdelbary A, Essam T, Abd EL-Salam RM, Aly Kassem AA, El-Salam RMA, *et al.* Niosomes as a potential drug delivery system for increasing the efficacy and safety of nystatin. Drug Dev Ind Pharm [Internet]. 2011 Dec 27 [cited 2017 Oct 13];37 (12):1491–508. Available from: http://www.ncbi.nlm.nih.gov/pubmed/21707323.
40. Attia IA, El-Gizawy SA, Fouda MA, Donia AM. Influence of a niosomal formulation on the oral bioavailability of acyclovir in rabbits. AAPS PharmSciTech. 2007;8(4):E106. https://doi.org/10.1208/pt0804106.
41. Arafa MG, Ayoub BM. DOE optimization of nano-based carrier of pregabalin as hydrogel: new therapeutic & chemometric approaches for controlled drug delivery systems. Sci Rep. 2017;7(January):41503. Nature Publishing Group.
42. Mokhtar M, Sammour OA, Hammad MA, Megrab NA. Effect of some formulation parameters on flurbiprofen encapsulation and release rates of niosomes prepared from proniosomes. Int J Pharm [Internet]. 2008 [cited 2014 Feb 11];361 (1–2):104–11. Available from: http://www.ncbi.nlm.nih.gov/pubmed/18577437.
43. Li Y, Zhao X, Zu Y, Zhang Y. Preparation and characterization of paclitaxel nanosuspension using novel emulsification method by combining high speed homogenizer and high pressure homogenization. Int J Pharm. 2015;490(1):324–33. https://doi.org/10.1016/j.ijpharm.2015.05.070.
44. Ahmed TA, El-Say KM, Aljaeid BM, Fahmy UA, Abd-Allah FI. Transdermal glimepiride delivery system based on optimized ethosomal nano-vesicles: preparation, characterization, in vitro,-ex vivo and clinical evaluation. Int Joumal Pharm [Internet]. Elsevier B.V.; 2016; 500 (1–2):245–54. Available from: http://linkinghub.elsevier.com/retrieve/pii/S0378517316300187.
45. Paolino D, Cosco D, Muzzalupo R, Trapasso E, Picci N, Fresta M. Innovative bola-surfactant niosomes as topical delivery systems of 5-fluorouracil for the treatment of skin cancer. Int J Pharm. 2008;353(1–2):233–42.
46. Mahmoudi Z, Upadhye S, Ferrizzi D, Rajabi-Siahboomi A. In vitro characterization of a novel polymeric system for preparation of amorphous solid drug dispersions. AAPS J. 2014;16(4):685–97. https://doi.org/10.1208/s12248-014-9590-y.
47. Shaker DS, Shaker MA, Hanafy MS. Cellular uptake, cytotoxicity and in-vivo evaluation of tamoxifen citrate loaded niosomes. Int J Pharm. 2015;493(1–2):285–94.
48. Danhier F, Lecouturier N, Vroman B, Jérôme C, Marchand-Brynaert J, Feron O, et al. Paclitaxel-loaded PEGylated PLGA-based nanoparticles: in vitro and in vivo evaluation. J Control Release. 2009;133(1):11–7. https://doi.org/10.1016/j.jconrel.2008.09.086. Elsevier BV.
49. Mulik RS, Mönkkönen J, Juvonen RO, Mahadik KR, Paradkar AR. ApoE3 mediated polymeric nanoparticles containing curcumin: apoptosis induced in vitro anticancer activity against neuroblastoma cells. Int J Pharm. 2012;437(1–2):29–41. Elsevier B.V.
50. El-Nabarawi MA, Bendas ER, El Rehem RTA, Abary MYS. Transdermal drug delivery of paroxetine through lipid-vesicular formulation to augment its bioavailability. Int J Pharm. 2013;443(1–2):307–17. Elsevier B.V.
51. Thakur V, Kush P, Pandey RS, Jain UK, Chandra R, Madan J. Vincristine sulfate loaded dextran microspheres amalgamated with thermosensitive gel offered sustained release and enhanced cytotoxicity in THP-1, human leukemia cells: in vitro and in vivo study. Mater Sci Eng C. 2016;61:113–22. https://doi.org/10.1016/j.msec.2015.12.015. Elsevier B.V.
52. Qadir A, Faiyazuddin MD, Talib Hussain MD, Alshammari TM, Shakeel F. Critical steps and energetics involved in a successful development of a stable nanoemulsion. J Mol Liq. 2016;214:7–18. https://doi.org/10.1016/j.molliq.2015.11.050. Elsevier BV.
53. Manconi M, Sinico C, Valenti D, Lai F, Fadda AM. Niosomes as carriers for tretinoin: III. A study into the in vitro cutaneous delivery of vesicle-incorporated tretinoin. Int J Pharm. 2006;311(1–2):11–9.
54. El-Ridy MS, AA AER, Awad GM, Khalil RM, Younis MM. In-vitro and in-vivo evaluation of niosomes containing celecoxib. Int J Pharm Sci Res. 2014;5(11):4677–88.
55. Ertekin ZC, Bayindir ZS, Yuksel N. Stability studies on piroxicam encapsulated niosomes. Curr Drug Deliv. 2015;12(2):192–9. https://doi.org/10.2174/1567201811666140723115852.
56. Zhang Y, Zhang K, Wu Z, Guo T, Ye B, Lu M, et al. Evaluation of transdermal salidroside delivery using niosomes via in vitro cellular uptake. Int J Pharm. 2015;478(1):138–46. https://doi.org/10.1016/j.ijpharm.2014.11.018. Elsevier BV.
57. Mosmann T. Rapid colorimetric assay for cellular growth and survival: application to proliferation and cytotoxicity assays. J Immunol Methods. 1983;65(1–2):55–63. https://doi.org/10.1016/0022-1759(83)90303-4.
58. Scudiero DA, Shoemaker RH, Paull KD, Monks A, Tierney S, Nofziger TH, et al. Evaluation of a soluble tetrazolium/formazan assay for cell growth and drug sensitivity in culture using human and other tumor cell lines. Cancer Res. 1988;48(17):4827–33.
59. Mahmoud AM, Al-Abd AM, Lightfoot DA, El-Shemy HA. Anti-cancer characteristics of mevinolin against three different solid tumor cell lines was not solely p 53-dependent. J Enzyme Inhib Med Chem [Internet]. 2012 [cited 2017 Oct 9];27(5):673–9. Available from: http://www.ncbi.nlm.nih.gov/pubmed/21883038.
60. Evans BC, Nelson CE, Yu SS, Beavers KR, Kim AJ, Li H, *et al.* Ex vivo red blood cell hemolysis assay for the evaluation of pH-responsive endosomolytic agents for cytosolic delivery of biomacromolecular drugs. J Vis Exp [Internet]. 2013 [cited 2016 Jun 29];73 (e50166):1–5. Available from: http://www.ncbi.nlm.nih.gov/pubmed/23524982.
61. Abdelkader H, Ismail S, Kamal A, Alany RG. Design and evaluation of controlled-release niosomes and discomes for naltrexone hydrochloride ocular delivery. J Pharm Sci. 2011;99(10):1833–46.
62. Guinedi AS, Mortada ND, Mansour S, Hathout RM. Preparation and evaluation of reverse-phase evaporation and multilamellar niosomes as ophthalmic carriers of acetazolamide. Int J Pharm [Internet]. 2005 Dec 8 [cited 2014 Nov 27];306 (1–2):71–82. Available from: http://www.ncbi.nlm.nih.gov/pubmed/16263229.
63. Nasr M, Mansour S, Mortada ND, Elshamy AA. Vesicular aceclofenac systems: a comparative study between liposomes and niosomes. J Microencapsul [Internet]. Informa UK Ltd UK; 2008 7 [cited 2014 Nov 27];25(7):499–512. Available from: http://informahealthcare.com/doi/abs/10.1080/02652040802055411.
64. Sahoo RK, Biswas N, Guha A, Sahoo N, Kuotsu K. Development and in vitro/in vivo evaluation of controlled release provesicles of a nateglinide–maltodextrin complex. Acta Pharm Sin B. 2014;4(5):408–16. https://doi.org/10.1016/j.apsb.2014.08.001. Elsevier.
65. Pezeshky A, Ghanbarzadeh B, Hamishehkar H, Moghadam M, Babazadeh A. Vitamin A palmitate-bearing nanoliposomes: preparation and characterization. Food Biosci. 2016;13:49–55. https://doi.org/10.1016/j.fbio.2015.12.002. Elsevier.
66. Traikia M, Warschawski DE, Recouvreur M, Cartaud J, Devaux PF. Formation of unilamellar vesicles by repetitive freeze-thaw cycles: characterization by electron microscopy and 31 P-nuclear magnetic resonance. Eur Biophys J. 2000;29(3):184–95.
67. Yoshida H, Lehr CM, Kok W, Junginger HE, Verhoef JC, Bouwstra JA. Niosomes for oral delivery of peptide drugs. J Control Release. 1992;21(1–3):145–53. https://doi.org/10.1016/0168-3659(92)90016-K.
68. Shaker DS, Shaker MA, Klingner A, Hanafy MS. In situ thermosensitive Tamoxifen citrate loaded hydrogels: an effective tool in breast cancer loco-regional therapy. J Drug Deliv Sci Technol. 2016;35:155–64. https://doi.org/10.1016/j.jddst.2016.05.007. Elsevier Ltd.

69. Moazeni E, Gilani K, Sotoudegan F, Pardakhty A, Najafabadi AR, Ghalandari R, et al. Formulation and in vitro evaluation of ciprofloxacin containing niosomes for pulmonary delivery. J Microencapsul. 2010;27(7):618–27. https://doi.org/10.3109/02652048.2010.506579.
70. Cortesi R, Esposito E, Corradini F, Sivieri E, Drechsler M, Rossi A, et al. Non-phospholipid vesicles as carriers for peptides and proteins: production, characterization and stability studies. Int J Pharm. 2007;339(1–2):52–60. https://doi.org/10.1016/j.ijpharm.2007.02.024.
71. Di Marzio L, Marianecci C, Petrone M, Rinaldi F, Carafa M. Novel pH-sensitive non-ionic surfactant vesicles: comparison between Tween 21 and Tween 20. Colloids Surfaces B Biointerfaces. 2011;82(1):18–24. https://doi.org/10.1016/j.colsurfb.2010.08.004. Elsevier BV.
72. Hashim F, El-Ridy M, Nasr M, Abdallah Y. Preparation and characterization of niosomes containing ribavirin for liver targeting. Drug Deliv. 2010;17(5):282–7. https://doi.org/10.3109/10717541003706257.
73. Muzzalupo R, Trombino S, Iemma F, Puoci F, La Mesa C, Picci N. Preparation and characterization of bolaform surfactant vesicles. Colloids Surfaces B Biointerfaces. 2005;46(2):78–83. https://doi.org/10.1016/j.colsurfb.2005.09.003.
74. Sathyavathi V, Hasansathali AA, Ilavarasan R, Sangeetha A. Formulation and evaluation of niosomal in situ gel ocular delivery system of brimonidine tartrate and hydrogels. Int J life Sci Pharm Res. 2012;2(1):L-82–95.
75. Pardakhty A, Varshosaz J, Rouholamini A. In vitro study of polyoxyethylene alkyl ether niosomes for delivery of insulin. Int J Pharm [Internet]. 2007 [cited 2014 Dec 17];328(2):130–41. Available from: http://www.ncbi.nlm.nih.gov/pubmed/16997517.
76. Aboelwafa AA, El-Setouhy DA, Elmeshad AN. Comparative study on the effects of some polyoxyethylene alkyl ether ?and sorbitan fatty acid ester surfactants on the performance of transdermal carvedilol proniosomal gel using experimental design. AAPS PharmSciTech [Internet]. 2010 Dec [cited 2014 Feb 19];11(4):1591–602. Available from: http://www.pubmedcentral.nih.gov/articlerender.fcgi?artid=3011071?&tool=pmcentrez&rendertype=abstract ?.
77. El-Laithy HM, Shoukry O, Mahran LG. Novel sugar esters proniosomes for transdermal delivery of vinpocetine: preclinical and clinical studies. Eur J Pharm Biopharm [Internet]. Elsevier B.V.; 2011 Jan [cited 2014 Apr 23];77(1):43–55. Available from: http://www.ncbi.nlm.nih.gov/pubmed/21056658.
78. Devaraj GN, Parakh SR, Devraj R, Apte SS, Rao BR, Rambhau D. Release studies on niosomes containing fatty alcohols as bilayer stabilizers instead of cholesterol. J Colloid Interface Sci. 2002;251(2):360–5. https://doi.org/10.1006/jcis.2002.8399.
79. Ruckmani K, Sankar V. Formulation and optimization of zidovudine niosomes. AAPS PharmSciTech. 2010;11(3):1119–27. https://doi.org/10.1208/s12249-010-9480-2.
80. Abdelbary G, El-Gendy N. Niosome-encapsulated gentamicin for ophthalmic controlled delivery. AAPS PharmSciTech [Internet]. 2008 Jan [cited 2014 Dec 4];9(3):740–7. Available from: http://www.pubmedcentral.nih.gov/articlerender.fcgi?artid=?2977028&tool=pmcentrez&rendertype=abstract.
81. Ferreira SLC, Bruns RE, Ferreira HS, Matos GD, David JM, Brandão GC, et al. Box-Behnken design: an alternative for the optimization of analytical methods. Anal Chim Acta. 2007;597(2):179–86. https://doi.org/10.1016/j.aca.2007.07.011.
82. Armengol X, Estelrich J. Physical stability of different liposome compositions obtained by extrusion method. J Microencapsul. 1995;12(5):525–35. https://doi.org/10.3109/02652049509006783.
83. Pokharkar VB, Mandpe LP, Padamwar MN, Ambike AA, Mahadik KR, Paradkar A. Development, characterization and stabilization of amorphous form of a low Tg drug. Powder Technol [Internet]. 2006 Sep [cited 2014 Oct 29];167(1):20–5. Available from: http://linkinghub.elsevier.com/retrieve/pii/S0032591006001732.
84. Hanaor D, Michelazzi M, Leonelli C, Sorrell CC. The effects of carboxylic acids on the aqueous dispersion and electrophoretic deposition of ZrO2. J Eur Ceram Soc. 2012;32(1):235–44. https://doi.org/10.1016/j.jeurceramsoc.2011.08.015. Elsevier Ltd.
85. Chaudhary PM, Roninson IB. Induction of multidrug resistance in human cells by transient exposure to different chemotherapeutic drugs. J Natl Cancer Inst [Internet]. 1993 Apr 21 [cited 2017 Oct 9];85(8):632–9. Available from: http://www.ncbi.nlm.nih.gov/pubmed/8096875.
86. Kern DH, Weisenthal LM. Highly specific prediction of antineoplastic drug resistance with an in vitro assay using suprapharmacologic drug exposures. J Natl Cancer Inst [Internet]. 1990 [cited 2017 Oct 9];82(7):582–8. Available from: http://www.ncbi.nlm.nih.gov/pubmed/2313735.
87. El-Araby ME, Omar AM, Khayat MT, Assiri HA, Al-Abd AM. Molecular mimics of classic P-glycoprotein inhibitors as multidrug resistance suppressors and their synergistic effect on paclitaxel. PLoS One [Internet]. Public Library of Science; 2017 [cited 2017 Oct 9];12(1):e0168938. Available from: http://www.ncbi.nlm.nih.gov/pubmed/28068430.
88. Chandratre SS, Dash AK. Multifunctional nanoparticles for prostate cancer therapy. Am Assoc Pharm Sci. 2015;16(1):98–107.
89. Mortazavi SM, Mohammadabadi MR, Khosravi-Darani K, Mozafari MR. Preparation of liposomal gene therapy vectors by a scalable method without using volatile solvents or detergents. J Biotechnol. 2007;129(4):604–13. https://doi.org/10.1016/j.jbiotec.2007.02.005.
90. Shenoy VS, Gude RP, Murthy RS. In vitro anticancer evaluation of 5-fluorouracil lipid nanoparticles using B16F10 melanoma cell lines. Int Nano Lett. 2013;3(1):36. https://doi.org/10.1186/2228-5326-3-36.
91. Tavano L, Aiello R, Ioele G, Picci N, Muzzalupo R. Niosomes from glucuronic acid-based surfactant as new carriers for cancer therapy: preparation, characterization and biological properties. Colloids Surfaces B Biointerfaces. 2014;118:7–13. Elsevier B.V.
92. Sharma V, Anandhakumar S, Sasidharan M. Self-degrading niosomes for encapsulation of hydrophilic and hydrophobic drugs: An efficient carrier for cancer multi-drug delivery. Mater Sci Eng C Mater Biol Appl [Internet]. Elsevier B.V.; 2015 Nov 1 [cited 2017 Oct 13];56:393–400. Available from: http://www.ncbi.nlm.nih.gov/pubmed/26249606.
93. Haley B, Frenkel E. Nanoparticles for drug delivery in cancer treatment. Urol Oncol Semin Orig Investig [Internet]. 2008 [cited 2017 Oct 9];26(1):57–64. Available from: http://www.ncbi.nlm.nih.gov/pubmed/18190833.